

IN-ORBIT ESTIMATION OF INERTIA AND MOMENTUM-ACTUATOR ALIGNMENT PARAMETERS

Michael C. Norman*, Mason A. Peck†, and Daniel J. O’Shaughnessy‡

Knowledge of the mass distribution and momentum actuator alignment parameters of a spacecraft is vital to the control of its attitude motion. The difficulty of measuring the complete set of these quantities prior to launch along with the potential for changes in the spacecraft mass distribution during operations suggests the utility of estimating these parameters in-orbit from available telemetry data. This paper develops a series of possible on-board parameter estimation schemes based on measurement equations describing the angular momentum and kinetic energy states of the rigid-body system. The performance of the algorithms is compared over both a simulated maneuver and a series of data sets from the MESSENGER spacecraft.

INTRODUCTION

Successful spacecraft attitude control and general operations are typically predicated upon knowledge of the mass distribution of the spacecraft and the alignment of relevant actuators. The mass distribution, in the form of a body-fixed inertia matrix, can be predicted to a limited extent by summing contributions from individual components on the basis of their assumed locations. This component-level knowledge, however, is not necessarily always available or accurate (e.g. in the cases of a broken appendage or of modeling fuel distribution, respectively). Modeling errors introduced in the form of an inaccurate mass distribution produce inaccurate predictions of attitude motion under feedback control, resulting in a mismatch between desired and actual spacecraft pointing performance. Residual attitude-actuator alignment errors after hardware integration and testing can similarly affect closed-loop pointing performance. Developing the capability to estimate these inertia parameters and actuator alignment errors in-orbit would not only aid in optimizing spacecraft pointing performance but also provide a means to diagnose erroneous or unexpected rigid-body attitude motion due to mass distribution changes, such as a failed deployment, or attitude actuator misalignments.

The literature suggests several approaches to estimating these parameters from spacecraft telemetry data. One general set of methods makes use of the rigid body attitude equations of motion

*Graduate Research Assistant, Department of Mechanical and Aerospace Engineering, Cornell University, 127 Upson Hall, Ithaca, NY 14853

†Assistant Professor, Department of Mechanical and Aerospace Engineering, Cornell University, 212 Upson Hall, Ithaca, NY 14853

‡Senior Staff, The Johns Hopkins Applied Physics Laboratory, Laurel, MD 20723

described by Euler's equation*.

$$[I] \dot{\omega} + [\omega^x] [I] \omega = \sum M \quad (1)$$

where $[\omega^x] = \begin{bmatrix} 0 & -\omega_3 & \omega_2 \\ \omega_3 & 0 & -\omega_1 \\ -\omega_2 & \omega_1 & 0 \end{bmatrix}$

Bergman, Walker, and Levy developed a second-order filter to extract rigid body inertia parameters a discrete form of equation (1) that neglected the gyroscopic term in the presence of known thruster inputs and external disturbances, and they tested it on simulated shuttle orbiter maneuvers.¹ Wilson, Sutter, and Mah similarly developed a filter producing inertia parameters and thruster modeling based on equation (1) but chose to include the gyroscopic term.² Thienel, Luquette, and Sanner developed an adaptive attitude control algorithm based on equation (1) that concurrently yields an estimate of the spacecraft inertia parameters.³ Fosbury and Nebelecky limited their approach to determining actuator alignment parameters in the presence of a known mass distribution noisy telemetry data.⁴ As noted by Fosbury and Nebelecky, methods using equation (1) as the basis for a measurement equation necessarily make use of the time derivative of the body rotation rate, $\dot{\omega}$, a quantity that must be derived from numerical differentiation. The amplification of noise introduced in this process limits the quality of the estimates produced.

Tanygin and Williams suggested a second approach to the problem of inertia parameter estimation that integrates a projection of the rigid body dynamics to produce an equation relating the rotational kinetic energy of the spacecraft at two times $\tau = 0$ and t to the work done by the actuator inputs.⁵

$$\frac{1}{2} \omega^T [I] \omega \Big|_t = T|_0 + \int_0^t \omega^T \sum M d\tau \quad (2)$$

This projection removes the gyroscopic term and allows for the inertia parameters to enter the measurement equation linearly, naturally lending itself to the formulation of a batch least-squares estimation problem. Tanygin and Williams successfully tested the algorithm on simulated and actual data produced by the Simplified Aid for EVA Rescue (SAFER) system.⁵ The algorithm depends, however, upon knowledge of the initial kinetic energy and the accuracy numerical integration scheme used to produce the work done by the torque inputs. Simple implementations of such a numerical integration technique requires a small, fixed time step between measurements, especially in the case of a recursive, on-board estimation scheme.

A third approach instead examines the angular momentum of the spacecraft, corresponding to the integral of equation (1) with respect to time. Under the specialized case where external torques can be neglected, the total angular momentum vector of the spacecraft remains inertially fixed:

$$[{}^N Q^k] \left([I] \omega + \sum I_{w,i} \Omega_i a_i \right) \Big|_j = [{}^N Q^j] \left([I] \omega + \sum I_{w,i} \Omega_i a_i \right) \Big|_k \quad (3)$$

Peck introduced the use of conservation of angular momentum, described by equation (3), as the basis of a batch least-squares estimator for spacecraft inertia parameters.⁶⁻⁸ The scheme operates by comparing the calculated momentum state at two distinct times and generating suitable inertia parameters by minimizing the resulting error. A distinct advantage of this approach over others is the ability to compare measurements with arbitrary temporal spacing. Peck extended this approach

*A section on mathematical notation is provided at the end of the paper.

by incorporating the gravity-gradient torque as a known external input.⁹ A version of a momentum-based approach with momentum actuators was successfully tested on Cassini flight data.¹⁰ Psiaki further developed this method by including reaction wheel and magnetic torquer alignment and scaling parameters, and he applied it to data from the Wilkinson Microwave Anisotropy Probe (WMAP) spacecraft.¹¹ Whereas Psiaki compared sequential angular velocity, spacecraft attitude, and actuator input states, in general, the optimal choice of time indices to compare in equation (3) is unclear: comparing states with large temporal separations may violate the assumption of conservation of angular momentum, but small separations may not provide sufficient information during coasting maneuvers.

This paper proposes a novel momentum-based estimation scheme for inertia and reaction-wheel alignment parameters that addresses several concerns raised by the above approaches. The scheme takes a recursive form and simultaneously estimates the momentum, inertia parameters, and actuator alignment in the presence of additive noise in the spacecraft attitude-dynamics states. Because the measurement equation that describes the angular momentum of the spacecraft is of a form similar to that of equation (3) rather than torque balance in the form of equation (1), no numerical time derivatives of wheel speeds or body rates are necessary, and non-uniform temporal separation between measurements is acceptable. Inclusion of the angular momentum state allows for the development of a measurement equation comparing the calculated angular momentum at a single time index to a simultaneously developed “optimal” angular momentum estimate.

Several variations of the parameter estimator are developed, incorporating different combinations of estimated states and measurement equations. The paper first describes the development of the estimation algorithm and then examines the performance of the proposed algorithm over a simulated maneuver and a series of calibration maneuver data sets from the MERcurey Surface, Space ENvironment, GEochemistry, and Ranging (MESSENGER) spacecraft. The paper ends with a summary of the algorithm performance and discussion of the results.

ALGORITHM DEVELOPMENT

Developing an estimation scheme first requires a suitable description of the measurements observed and the dynamics equations describing the estimator-state time evolution. In the case of the inertia and actuator alignment parameter estimation problem, the state dynamics are modeled as a discrete-time system, allowing for the implementation of several standard sub-optimal filtering approaches, such as an Extended Kalman Filter (EKF) or Extended Square-Root Information Filter (ESRIF):

$$\begin{aligned}
 x_e(k+1) &= f(x_e(k), u(k), v(k)) \\
 &\approx f(\bar{x}_e(k), u(k), 0) + \left[\frac{\partial f}{\partial x_e} \right]_k (x_e(k) - \bar{x}_e(k)) + \left[\frac{\partial f}{\partial v} \right]_k v(k) \quad (4) \\
 z_e(k) &= H(x_e(k), w(k)) \\
 &\approx H(\bar{x}_e(k), 0) + \left[\frac{\partial H}{\partial x_e} \right]_k (x_e(k) - \bar{x}_e(k)) + \left[\frac{\partial H}{\partial w} \right]_k w(k)
 \end{aligned}$$

In addition to the momentum-based inertia and actuator-alignment parameter estimator, four other estimation schemes are developed for comparison. The first of these corresponds to a recursive formulation of an inertia estimation scheme using only the rotational kinetic energy equation from equation (2). As the measurement equation for this estimator is independent of the actuator axes,

the actuator-alignment error parameters are not included in this estimator. The second variation estimates only the angular momentum and inertia parameters, effectively assuming that the actuator alignment is known precisely. The third estimation scheme includes both angular momentum and energy measurements and states along with inertia parameter states. The fourth variant similarly incorporates both the angular momentum and rotational kinetic energy measurements and states to estimate both the inertia and actuator-alignment parameters. The original estimation scheme and these four variants are all composed of different combinations of the same base set of measurement equations (angular momentum and rotational kinetic energy) and estimation states (h, T, \tilde{I}, P) .

Table 1. Estimator scheme descriptions

	Base	Variant 1	Variant 2	Variant 3	Variant 4
Estimator state	$\begin{bmatrix} h \\ \tilde{I} \\ P \end{bmatrix}$	$\begin{bmatrix} T \\ \tilde{I} \end{bmatrix}$	$\begin{bmatrix} h \\ \tilde{I} \end{bmatrix}$	$\begin{bmatrix} h \\ T \\ \tilde{I} \end{bmatrix}$	$\begin{bmatrix} h \\ T \\ \tilde{I} \\ P \end{bmatrix}$
Measurements	h	T	h	h, T	h, T

The body rates and reaction-wheel speeds reported in the telemetry data are assumed to be corrupted by additive, zero-mean noise that follows a normal distribution. Similarly, the direction cosine matrix ${}^kQ^N$ describing the attitude of the spacecraft with respect to an inertial reference is assumed to be multiplied by an error rotation matrix that can be represented as a small-angle rotation about an arbitrary axis:

$$\begin{aligned}
 \Omega(k) &= \bar{\Omega}(k) + \Delta\Omega(k) & \Delta\Omega(k) &\sim \mathcal{N}(0, \sigma_\Omega^2 [1_n]) \\
 \omega(k) &= \bar{\omega}(k) + \Delta\omega(k) & \Delta\omega(k) &\sim \mathcal{N}(0, \sigma_\omega^2 [1_3]) \\
 {}^kQ^N &= [\Delta Q(k)] [{}^k\bar{Q}^n] \approx ([1_3] - [\Delta\theta^x(k)]) [{}^k\bar{Q}^N] & \Delta\theta(k) &\sim \mathcal{N}(0, \sigma_\theta^2 [1_3])
 \end{aligned} \tag{5}$$

Measurement Equations

In the absence of external torques, the total angular momentum of the spacecraft remains inertially fixed and is determined by the sum of contributions from the spacecraft bus and momentum actuators. Because the body rates and reaction-wheel speeds are reported in body-fixed coordinates, the calculation incorporates the spacecraft attitude with respect to inertially fixed reference coordinates to rotate the angular momentum to the body-fixed coordinates.

$$z_h(k) = 0 = [I] \omega(k) - [{}^kQ^N] h + \sum I_{w,i} \Omega_i(k) a_i \tag{6}$$

Linearizing equation (6) about current estimates of the angular momentum, inertia, and actuator alignment parameters, along with the descriptions of \bar{a}_i and $[\partial a_i / \partial p_i]$ (see Appendix) equations(23)

and (24), reformats the measurement to match equation (4):

$$z_h(k) \approx \bar{z}_h(k) + \begin{bmatrix} - [{}^k\bar{Q}^N] & [\tilde{\omega}(k)] & I_{w,1}\bar{\Omega}_1 \left[\frac{\partial a_1}{\partial p_1} \right]_k & \cdots & I_{w,n}\bar{\Omega}_n \left[\frac{\partial a_n}{\partial p_n} \right]_k \end{bmatrix} \left(\begin{bmatrix} \bar{h} \\ \tilde{I} \\ P \end{bmatrix} - \begin{bmatrix} \bar{h}(k) \\ \tilde{I}(k) \\ \bar{P}(k) \end{bmatrix} \right) + \begin{bmatrix} - \left([{}^k\bar{Q}^N] \bar{h}(k) \right)^x & [\bar{I}(k)] & I_{w,1}\bar{a}_1(k) & \cdots & I_{w,n}\bar{a}_n(k) & [1_3] \end{bmatrix} \begin{bmatrix} \Delta\theta \\ \Delta\omega \\ \Delta\Omega \\ w_h \end{bmatrix} \quad (7)$$

$$\text{where } \bar{z}_h(k) = [\bar{I}(k)] \bar{\omega}(k) - [{}^k\bar{Q}^N] \bar{h}(k) + \sum I_{w,i}\bar{\Omega}_i(k) \bar{a}_i(k)$$

$$\text{and } [\tilde{\omega}(k)] = \begin{bmatrix} \bar{\omega}_1(k) & 0 & 0 & \bar{\omega}_2(k) & \bar{\omega}_3(k) & 0 \\ 0 & \bar{\omega}_2(k) & 0 & \bar{\omega}_1(k) & 0 & \bar{\omega}_3(k) \\ 0 & 0 & \bar{\omega}_3(k) & 0 & \bar{\omega}_1(k) & \bar{\omega}_2(k) \end{bmatrix}$$

For the estimation schemes that do not include the actuator-alignment parameters in the estimated state, the relevant columns of the matrices in equation (7) are not included. The w_h term is included as an optional additional source of noise in the angular momentum equation to help account for errors introduced by linearization.

The rotational kinetic energy of the spacecraft bus has a simple form depending only on the angular velocity of the spacecraft:

$$z_T(k) = 0 = T - \frac{1}{2} \omega^T(k) [I] \omega(k) \quad (8)$$

The estimator states included in equation (8) enter linearly. Noise in the angular velocity knowledge and additional measurement noise can be incorporated by linearizing about the current inertia estimate and adding the term $w_T(k)$ as an optional source of additional measurement noise:

$$z_T(k) \approx T - \frac{1}{2} \bar{\omega}^T(k) [I] \bar{\omega}(k) - \bar{\omega}^T(k) [\bar{I}(k)] \Delta\omega(k) + w_T(k) \quad (9)$$

Equation 9 can similarly be reformatted to match the measurement equation (4):

$$0 = \begin{bmatrix} 1 & -\frac{1}{2} [\hat{\omega}(k)] \end{bmatrix} \begin{bmatrix} T \\ \tilde{I} \end{bmatrix} + \begin{bmatrix} -\bar{\omega}^T(k) [\bar{I}(k)] & 1 \end{bmatrix} \begin{bmatrix} \Delta\omega \\ w_T \end{bmatrix} \quad (10)$$

$$\text{where } [\hat{\omega}(k)] = [\bar{\omega}_1^2(k) \quad \bar{\omega}_2^2(k) \quad \bar{\omega}_3^2(k) \quad 2\bar{\omega}_1(k)\bar{\omega}_2(k) \quad 2\bar{\omega}_1(k)\bar{\omega}_3(k) \quad 2\bar{\omega}_2(k)\bar{\omega}_3(k)]$$

As the actuator alignment parameters do not appear in the measurement equation (10), they cannot be incorporated into an estimation scheme that uses only the rotational kinetic energy of the spacecraft as the basis for a measurement equation.

Discrete-Time Dynamics

Although several of the estimation state components are nominally constant parameters associated with the spacecraft attitude dynamics, making the assumption that they are modified by artificial process noise in the estimator formulation helps prevent the estimates from converging too

quickly and not incorporating subsequent measurements.^{1,12} This inclusion has the added benefit of allowing these supposed constants to be slowly time-varying. In the case of the inertia and actuator-alignment parameters, this flexibility could help model unexpected variations in the spacecraft mass distribution or configuration. In the absence of external torques, the total angular momentum of the spacecraft expressed in inertial coordinates, h , is time invariant. The addition of the artificial process noise to the angular momentum state dynamics, however, partially accounts for unmodeled external environmental torques:

$$\begin{aligned}\tilde{I}(k+1) &= \tilde{I}(k) + v_I(k) \\ P(k+1) &= P(k) + v_P(k) \\ h(k+1) &= h(k) + v_h(k)\end{aligned}\tag{11}$$

The rotational kinetic energy state evolves based on the inputs to the reaction wheels. Projecting equation (1) onto the body-rate vector, ω , describes the continuous-time dynamics of the rotational kinetic energy:

$$\dot{T}(k) = \omega^T(k) [I] \dot{\omega}(k) = -\omega^T(k) \sum I_{w,i} \dot{\Omega}_i a_i\tag{12}$$

Integrating between times t_k and t_{k+1} translates the continuous-time dynamics into a discrete-time form:

$$T(k+1) = T(k) - \int_{t_k}^{t_{k+1}} \omega^T \left(\sum I_{w,i} \dot{\Omega}_i a_i \right) dt\tag{13}$$

The integral in equation (13) requires continuous-time knowledge of ω and $\dot{\Omega}$. In practice, the attitude-dynamics states are known only at discrete times, and the reaction-wheel accelerations, $\dot{\Omega}$, need to be approximated from a known Ω time history, resulting in an approximation of the integral. The required fidelity of the particular integration scheme implemented depends largely on the sampling frequency of the available attitude-dynamics data.

$$\int_{t_k}^{t_{k+1}} \omega^T \left(\sum I_{w,i} \dot{\Omega}_i a_i \right) dt \approx \mathcal{J}(\omega, \Omega, a_1, \dots, a_n)\tag{14}$$

Linearizing equation (14) about the measured attitude-dynamics states, specifically $\bar{\omega}$ and $\bar{\Omega}$, allows for the appropriate incorporation of noise in the body-rate and reaction-wheel speed measurements into the discrete-time dynamics equation. Additional process noise, v_T , can be incorporated to help minimize the errors introduced with the integration approximation of equation (14):

$$\begin{aligned}T(k+1) \approx \bar{T}(k) - \mathcal{J}(\bar{\omega}, \bar{\Omega}, \bar{a}_1(k), \dots, \bar{a}_n(k)) &+ \begin{bmatrix} 1 & - \left[\frac{\partial \mathcal{J}}{\partial P} \right]_k \end{bmatrix} \left(\begin{bmatrix} T \\ P \end{bmatrix} - \begin{bmatrix} \bar{T}(k) \\ \bar{P}(k) \end{bmatrix} \right) \\ &+ \begin{bmatrix} - \left[\frac{\partial \mathcal{J}}{\partial \omega} \right]_k & - \left[\frac{\partial \mathcal{J}}{\partial \Omega} \right]_k & 1 \end{bmatrix} \begin{bmatrix} \Delta \omega \\ \Delta \Omega \\ v_T \end{bmatrix}\end{aligned}\tag{15}$$

The partial derivatives of \mathcal{J} included in equation (15) are dependent on the numerical differentiation scheme utilized to produce $\dot{\Omega}$ and the numerical integration scheme used to approximate the integral of equation (14).

REPRESENTATIVE ALGORITHM PERFORMANCE

Examination of the performance of the parameter estimators described by Table 1 over a computer-generated attitude dynamics history in a situation where the true parameter values are known provides a basis for comparison of the performance of the various schemes. Two sets of initial conditions were evaluated over the simulated maneuver for each of the estimation schemes. These schemes were implemented as an EKF and utilized trapezoidal integration to approximate the changes in the rotational kinetic energy state due to momentum actuator inputs given by equation (14) where appropriate. The parameter estimators were also applied to four sets of telemetry data from the MESSENGER spacecraft gathered during calibration maneuvers as examples of algorithm performance with actual data.

Performance with Simulated Data

The computer-generated attitude dynamics was based on the assumption of a rigid spacecraft with no applied external torques. The rigid body assumption neglects momentum and energy contributions from sources potentially included in higher-fidelity models, such as the effects of flexible structural modes or fuel slosh. The lack of external torques allows for the direct comparison of the momentum vector in inertial coordinates between two arbitrary times without needing to numerically integrate an input torque. Similarly, this simplification is equivalent to assuming that the only changes to the spacecraft rotational kinetic energy originate from the known momentum actuator inputs. Tanygin and Williams and later Peck addressed the incorporation of general external torques to energy- and angular momentum-based inertia estimation methods, respectively.^{5,9} In the performance evaluation here, measurements of the simulated wheel speeds, body rates, and attitude parameterization were assumed to be corrupted by noise in as described by (5). The relevant physical parameters of the simulated spacecraft are given in Table 2.

Table 2. Parameters for computer-generated attitude dynamics data

Inertia parameters in body coordinates ($kg \cdot m^2$)	True actuator axes in body coordinates	Wheel inertias ($kg \cdot m^2$)
$\begin{bmatrix} 308.5 & -0.1 & 0.0 \\ -0.1 & 402.1 & 4.5 \\ 0.0 & 4.5 & 508.8 \end{bmatrix}$	$\begin{bmatrix} 0.7379 & -0.7025 & 0.7429 & -0.7412 \\ 0.4719 & 0.5204 & -0.4790 & -0.5142 \\ 0.4825 & 0.4854 & 0.4675 & 0.4315 \end{bmatrix}$	$\begin{bmatrix} 0.012172 \\ 0.012274 \\ 0.012115 \\ 0.012298 \end{bmatrix}$

The simulated maneuver consisted of a sequence of commanded rotations about spacecraft body axes with interspersed rotations about linear combinations of two body axes. Figure 1 shows the time histories of the computer-generated attitude, angular velocity, and wheel speed components. Pittelkau and O’Shaughnessy utilized a similar maneuver to estimate the gyro misalignment for the MESSENGER spacecraft.¹³ The parameter estimation algorithms here were evaluated using the simulated maneuver and two sets of initial state estimates.

The first set of initial state estimates was based on the presumption of little knowledge of the angular momentum, energy, or inertia parameters but accurate knowledge of the actuator axes. The expectation was that this state would represent the ideal case for all the variants of the parameter

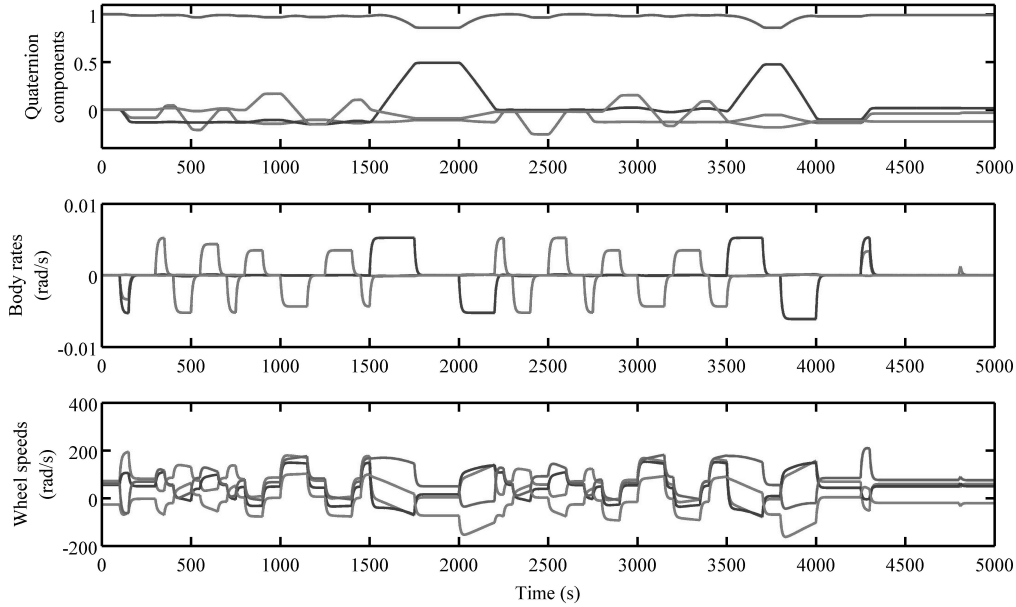


Figure 1. Computer-generated attitude-dynamics time histories for a sample maneuver.

estimators, as no errors due to actuator misalignment would be introduced into the algorithms incapable of appropriately compensating for them. Figures 2 and 3 respectively compare the magnitude of the inertia and alignment parameter errors across the implemented estimation schemes. Because only the “Base” and “Variant 4” estimation schemes from Table 1 include the actuator alignment parameter states, they are the only two compared in Fig. 3.

As demonstrated in Fig. 2, all five estimation schemes are capable of producing highly accurate estimates of the moments and products of inertia of a rigid body spacecraft. The estimators Variant 2 and Variant 3 converged to the true inertia parameters faster than the other schemes. These two variants did not include the actuator-alignment parameters as an estimated state but did include the angular momentum. Variant 3 also included the rotational kinetic energy measurement and state. These results suggest that including the angular momentum state and measurement improved the rate of convergence for the inertia parameters, but the performance of the algorithms was insensitive to the inclusion of the rotational kinetic energy. Inclusion of the alignment parameters, corresponding to the Base and Variant 4 estimators, resulted in comparatively worse performance, with Variant 4 producing the better of the two estimates of the inertia parameters. Similar results are seen in Fig. 3, where Variant 4 results in slightly lower error in the actuator alignment parameters.

The second set of initial state estimates incorporated similar assumptions regarding the inertia, angular momentum, and rotational kinetic energy states but introduced an error in the form of an incorrect initial estimate of the actuator axes. This error was expected to result in poor inertia parameter estimates for the estimation schemes that did not include the actuator-alignment parameters as estimator states. The error in the initial actuator-axis estimates correspond to angular offsets of 3.3355° , 4.2198° , 2.3492° , and 0.9645° from their true directions. Figures 4 and 5, respectively, compare the magnitude of the inertia and alignment-parameter errors across the implemented esti-

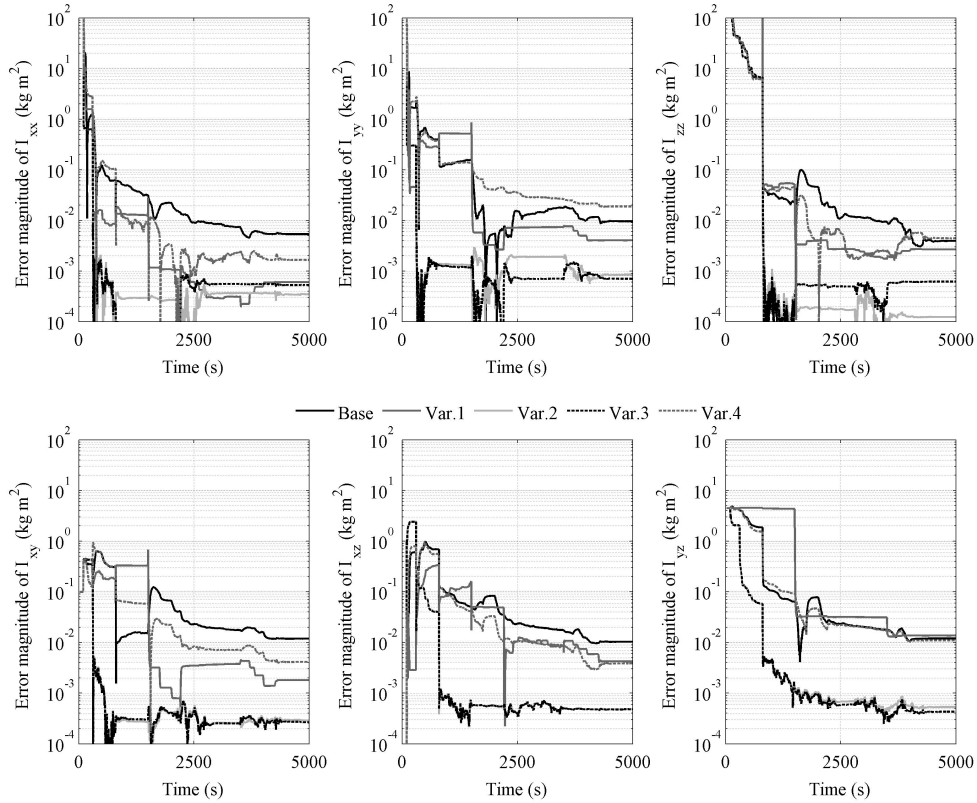


Figure 2. Estimated inertia parameters for simulated maneuver and accurate actuator-axis knowledge.

mation schemes. As expected, Fig. 4 demonstrates the error introduced by inaccurate actuator-axis knowledge into the inertia parameter estimates. These errors appear in the state estimates produced by the Variant 1, Variant 2, and Variant 3 estimation schemes. The ‘Base’ and ‘Variant 4’ estimates performed nearly equivalently, reducing the estimation error to a level comparable to that seen in Fig. 2. The Base and Variant 4 estimator configurations quickly converged to the correct actuator alignment parameters, as demonstrated in Fig. 5.

The final parameter and estimated standard deviations estimates produced by the different filter configurations for the two initial conditions sets and the simulated maneuver are detailed in Tables 3 and 4. All filter variations performed well when the momentum actuator axes were known *a priori*. Introducing error into this initial guess, however, results in substantial errors in the inertia parameter estimates of the filters that do not include actuator-alignment error in the estimated state. Compounding the issue, the estimated standard deviations of the inertia parameters produced by these filters do not reflect this error, indicating that the filters are falsely confident of their final outputs. The filters estimating the actuator misalignment parameters, however, still produce accurate inertia parameter estimates along with the true momentum actuator axes.

Table 3. Inertia parameter estimates produced by filters from simulated maneuver

Truth	Initial Estimate and Filter Configurations											
	Initial Estimate Set 1						Initial Estimate Set 2					
	Base	Var. 1	Var. 2	Var. 3	Var. 4	Base	Var. 1	Var. 2	Var. 3	Var. 4		
I_{xx}	380.5	380.5	380.5	380.5	380.5	380.5	390.0	389.7	389.8	380.5		
I_{yy}	402.1	402.1	402.1	402.1	402.1	402.0	406.6	404.6	405.2	402.0		
I_{zz}	508.8	508.8	508.8	508.8	508.8	508.9	470.0	471.2	470.7	508.9		
I_{xy}	-0.1	-0.1	-0.1	-0.1	-0.1	-0.1	-4.7	-3.2	-3.2	-0.1		
I_{xz}	0.0	0.0	0.0	0.0	0.0	-0.0	-11.6	-7.3	-7.3	0.0		
I_{yz}	4.5	4.5	4.5	4.5	4.5	4.5	-7.6	-3.2	-3.3	4.5		
$\sigma_{I_{xx}}$	-	0.207	0.140	0.092	0.070	0.208	0.140	0.092	0.070	0.193		
$\sigma_{I_{yy}}$	-	0.541	0.137	0.090	0.072	0.540	0.137	0.090	0.072	0.498		
$\sigma_{I_{zz}}$	-	0.465	0.202	0.103	0.090	0.467	0.202	0.103	0.090	0.418		
$\sigma_{I_{xy}}$	-	0.351	0.207	0.063	0.060	0.351	0.207	0.063	0.060	0.284		
$\sigma_{I_{xz}}$	-	0.403	7.723	0.068	0.068	0.404	7.723	0.068	0.068	0.336		
$\sigma_{I_{yz}}$	-	0.366	0.632	0.067	0.066	0.365	0.632	0.067	0.066	0.314		

Table 4. Actuator-axis estimates produced by filters from simulated maneuver

	Initial Estimate and Filter Configurations				
	Truth	Initial Estimate Set 1		Initial Estimate Set 2	
		Base	Var. 4	Base	Var. 4
a_{1x}	0.7379	0.7379	0.7379	0.7380	0.7380
a_{1y}	0.4719	0.4719	0.4719	0.4718	0.4718
a_{1z}	0.4825	0.4825	0.4825	0.4824	0.4825
a_{2x}	-0.7025	-0.7025	-0.7025	-0.7025	-0.7025
a_{2y}	0.5204	0.5204	0.5204	0.5203	0.5204
a_{2z}	0.4854	0.4855	0.4854	0.4856	0.4855
a_{3x}	0.7429	0.7429	0.7429	0.7429	0.7429
a_{3y}	-0.4790	-0.4790	-0.4790	-0.4789	-0.4789
a_{3z}	0.4675	0.4675	0.4675	0.4677	0.4676
a_{4x}	-0.7412	-0.7412	-0.7411	-0.7412	-0.7412
a_{4y}	-0.5142	-0.5142	-0.5143	-0.5142	-0.5142
a_{4z}	0.4315	0.4315	0.4316	0.4316	0.4316
σ_{p11}	-	0.2566	0.2297	0.2545	0.2286
σ_{p12}	-	0.6653	0.5453	0.6664	0.5444
σ_{p21}	-	0.2918	0.2595	0.2915	0.2594
σ_{p22}	-	0.7841	0.6353	0.7859	0.6378
σ_{p31}	-	0.4222	0.3527	0.4229	0.3521
σ_{p32}	-	0.2742	0.2456	0.2742	0.2465
σ_{p41}	-	0.2588	0.2241	0.2591	0.2250
σ_{p42}	-	0.2349	0.2184	0.2348	0.2184

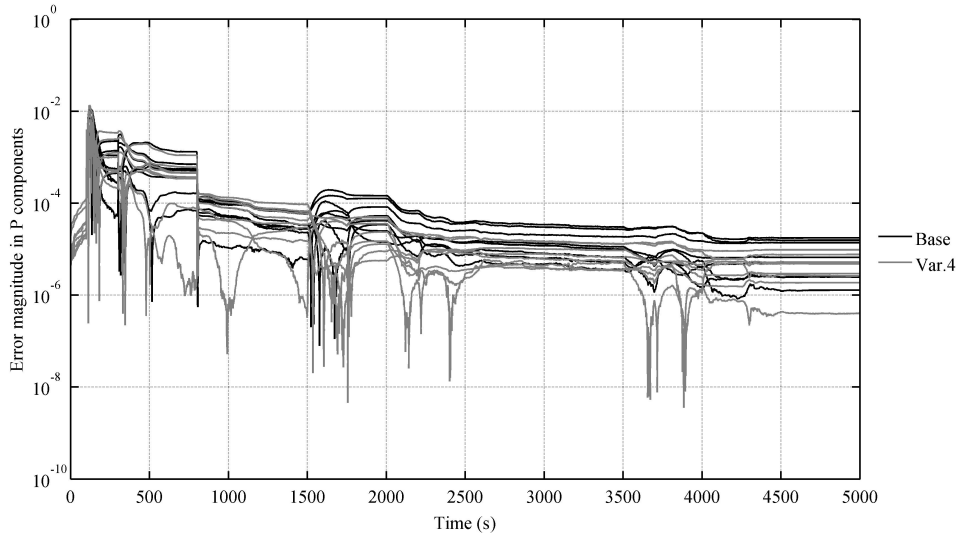


Figure 3. Estimated alignment parameters for simulated maneuver and accurate actuator-axis knowledge.

Performance with MESSENGER Data

The MESSENGER spacecraft launched on August 3, 2004, and is scheduled to enter in orbit Mercury in March 2011. Flight operations to date have included several attitude maneuvers designed to improve star tracker and gyro alignment knowledge.¹³ At each of the four maneuvers considered, an estimate of the inertia parameters of the spacecraft is available from pre-launch knowledge of the mechanical properties and location of individual rigid components and fuel. The presumed mechanical alignment of the reaction wheels is also available. The filter configurations described by Table 1 used the telemetry data generated by these maneuvers to form estimates of the inertia parameters and momentum-actuator axes. Tables 5 and 6 describe the final state estimates of the inertia and actuator-axis parameters along with their filter-produced standard deviations.

The estimation schemes that include the angular momentum state and measurement equation resulted in reasonably consistent inertia parameter estimates. The Variant 1 scheme, however, which made use only of the rotational kinetic energy measurement and state, produced significantly different inertia parameter estimates and larger standard deviations for those parameters. Comparing the final estimates of the momentum-based filters with actuator alignment parameter states to those without reveals little variation in the estimates between these filter configurations. The Base, Variant 2, Variant 3, and Variant 4 filters also produced similar inertia parameter estimates across the two-day separation between the calibration maneuvers performed on days 182 and 184 of 2008. As the assumed inertia parameters were identical for these two maneuvers, the consistency of the filter-produced estimates for the two data sets suggest that these inertia parameter estimation methods are reliable. The final estimate actuator axes of the Base and Variant 4 estimation schemes are also relatively consistent across all four calibration maneuvers. Because the axes of rotation of these momentum actuators are ideally considered fixed in the spacecraft's body frame, the similarity between these estimates also supports the accuracy of the filtering methods producing them.

The observed deviations of the inertia parameters, most noticeably the I_{yy} and I_{zz} terms, from the

Table 5. Inertia parameter estimates produced by filters from MESSENGER data

Calibration Maneuver Date and Filter Configurations												
2007 Day 262						2008 Day 182						
	Mech.	Base	Var.1	Var.2	Var.3	Var.4	Mech.	Base	Var.1	Var.2	Var.3	Var.4
I_{xx}	429.0	435.9	409.3	436.5	436.5	435.9	399.5	406.7	369.4	405.9	405.9	406.7
I_{yy}	427.2	438.5	420.0	438.2	438.2	438.5	404.8	430.4	409.1	430.4	430.4	430.4
I_{zz}	537.6	536.4	510.5	534.8	534.8	536.4	527.9	507.0	487.8	511.0	511.0	507.0
I_{xy}	-0.1	-3.9	8.2	-5.2	-5.2	-3.9	-0.1	-4.3	1.9	-3.3	-3.3	-4.3
I_{xz}	0.0	-0.2	-1.1	0.2	0.2	-0.2	0.0	0.2	-0.5	0.3	0.3	0.1
I_{yz}	4.2	5.0	-4.7	10.0	10.0	5.0	4.5	6.2	-1.0	8.7	8.7	6.2
σI_{xx}	-	0.106	9.321	0.097	0.097	0.106	-	0.116	8.305	0.093	0.093	0.116
σI_{yy}	-	0.134	8.379	0.064	0.064	0.134	-	0.171	8.429	0.064	0.064	0.171
σI_{zz}	-	0.149	15.62	0.112	0.112	0.149	-	0.231	14.69	0.110	0.110	0.231
σI_{xy}	-	0.070	9.584	0.053	0.053	0.070	-	0.063	9.252	0.053	0.053	0.063
σI_{xz}	-	0.088	9.966	0.073	0.073	0.088	-	0.088	9.969	0.071	0.071	0.088
σI_{yz}	-	0.100	9.886	0.056	0.056	0.100	-	0.100	9.983	0.055	0.055	0.100
2008 Day 184						2009 Day 222						
	Mech.	Base	Var.1	Var.2	Var.3	Var.4	Mech.	Base	Var.1	Var.2	Var.3	Var.4
I_{xx}	399.5	407.4	393.1	406.7	406.7	407.4	308.5	389.3	355.8	389.1	389.1	389.3
I_{yy}	404.8	432.3	423.9	431.2	431.2	432.3	402.1	428.1	410.4	428.5	428.5	428.1
I_{zz}	527.9	506.9	500.0	512.0	512.0	506.9	508.8	494.8	469.6	496.0	496.0	494.8
I_{xy}	-0.1	-4.0	-2.5	-2.9	-2.9	-4.0	-0.1	-2.8	0.7	-2.7	-2.7	-2.8
I_{xz}	0.0	-0.0	0.7	0.2	0.2	-0.0	0.0	1.4	1.3	0.3	0.3	1.4
I_{yz}	4.5	4.7	0.5	6.9	6.9	4.7	4.5	6.1	0.4	7.1	7.1	6.1
σI_{xx}	-	0.110	8.312	0.093	0.093	0.110	-	0.116	9.060	0.097	0.097	0.116
σI_{yy}	-	0.165	8.499	0.064	0.064	0.165	-	0.176	7.905	0.065	0.065	0.176
σI_{zz}	-	0.191	14.63	0.111	0.111	0.191	-	0.200	14.97	0.111	0.111	0.200
σI_{xy}	-	0.064	9.253	0.053	0.053	0.064	-	0.066	9.990	0.054	0.054	0.066
σI_{xz}	-	0.087	9.957	0.071	0.071	0.087	-	0.091	9.992	0.073	0.073	0.091
σI_{yz}	-	0.105	9.968	0.055	0.055	0.105	-	0.104	9.990	0.056	0.056	0.104

Table 6. Actuator axes estimates produced by filters from MESSENGER data

Mech.		Calibration Maneuver Date and Filter Configurations															
		2007 Day 262				2008 Day 182				2008 Day 184				2009 Day 2009			
		Base	Var. 4	Base	Var. 4	Base	Var. 4	Base	Var. 4	Base	Var. 4	Base	Var. 4				
a_{1x}	0.7500	0.7535	0.7535	0.7545	0.7545	0.7545	0.7561	0.7561	0.7561	0.7561	0.7582	0.7582					
a_{1y}	0.5000	0.5013	0.5013	0.5004	0.5004	0.5004	0.4988	0.4988	0.4988	0.4988	0.4885	0.4885					
a_{1z}	0.4330	0.4254	0.4254	0.4246	0.4246	0.4246	0.4237	0.4237	0.4237	0.4237	0.4318	0.4318					
a_{2x}	-0.7500	-0.7510	-0.7510	-0.7559	-0.7559	-0.7559	-0.7565	-0.7565	-0.7565	-0.7565	-0.7522	-0.7522					
a_{2y}	0.5000	0.5068	0.5068	0.4996	0.4996	0.4996	0.4940	0.4940	0.4940	0.4940	0.5023	0.5023					
a_{2z}	0.4330	0.4232	0.4232	0.4231	0.4231	0.4231	0.4287	0.4287	0.4287	0.4287	0.4264	0.4264					
a_{3x}	0.7500	0.7406	0.7406	0.7520	0.7520	0.7520	0.7523	0.7523	0.7523	0.7523	0.7498	0.7498					
a_{3y}	-0.5000	-0.5033	-0.5033	-0.5003	-0.5003	-0.5003	-0.5046	-0.5046	-0.5046	-0.5046	-0.5020	-0.5020					
a_{3z}	0.4330	0.4452	0.4452	0.4291	0.4291	0.4291	0.4236	0.4236	0.4236	0.4236	0.4310	0.4310					
a_{4x}	-0.7500	-0.7492	-0.7492	-0.7440	-0.7440	-0.7440	-0.7401	-0.7401	-0.7401	-0.7401	-0.7455	-0.7455					
a_{4y}	-0.5000	-0.4922	-0.4922	-0.5006	-0.5006	-0.5006	-0.5089	-0.5089	-0.5089	-0.5089	-0.5033	-0.5033					
a_{4z}	0.4330	0.4433	0.4433	0.4425	0.4425	0.4425	0.4396	0.4396	0.4396	0.4396	0.4369	0.4369					
σ_{p11}	-	0.7798	0.7798	0.9733	0.9733	0.9733	0.9315	0.9315	0.9315	0.9315	0.8147	0.8147					
σ_{p12}	-	0.9307	0.9307	0.9876	0.9876	0.9876	0.9824	0.9824	0.9824	0.9824	0.8564	0.8564					
σ_{p21}	-	0.5634	0.5634	0.8675	0.8675	0.8675	0.8257	0.8257	0.8257	0.8257	0.7513	0.7513					
σ_{p22}	-	0.7453	0.7453	0.8720	0.8720	0.8720	0.8756	0.8756	0.8756	0.8756	0.7977	0.7977					
σ_{p31}	-	0.7293	0.7293	0.7887	0.7887	0.7887	0.7255	0.7255	0.7255	0.7255	0.8625	0.8625					
σ_{p32}	-	0.7515	0.7515	0.8425	0.8425	0.8425	0.7598	0.7598	0.7598	0.7598	0.8896	0.8896					
σ_{p41}	-	0.7597	0.7597	0.7892	0.7892	0.7892	0.7120	0.7120	0.7120	0.7120	1.0499	1.0499					
σ_{p42}	-	0.6562	0.6562	0.8488	0.8488	0.8488	0.7418	0.7418	0.7418	0.7418	1.0934	1.0934					

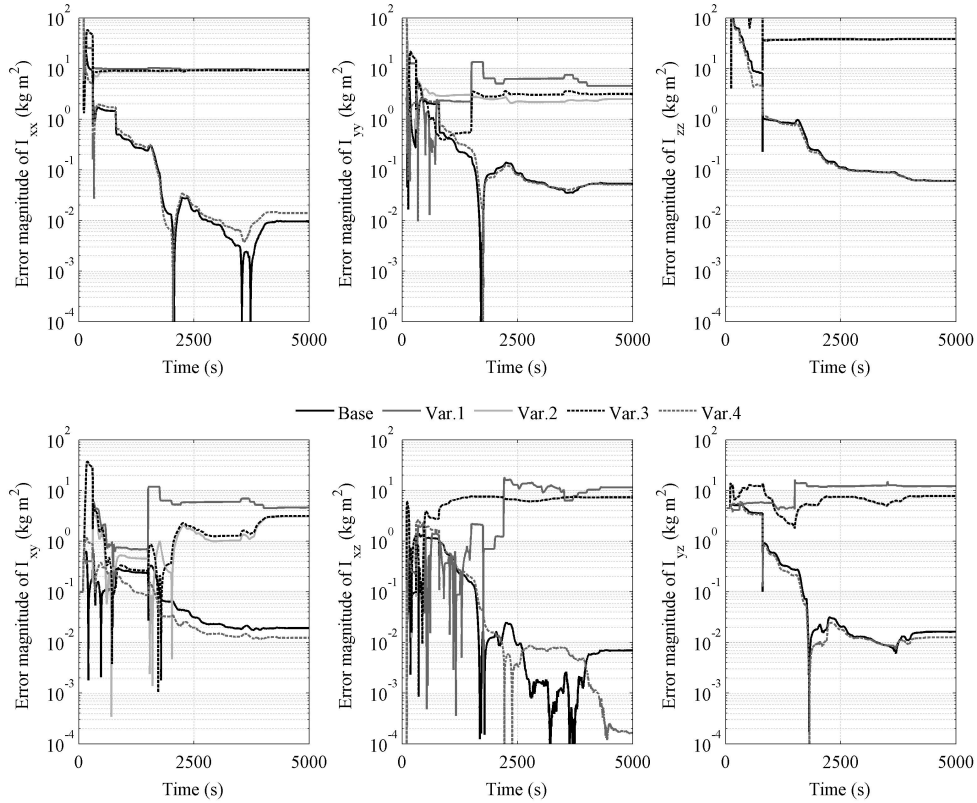


Figure 4. Estimated inertia parameters for simulated maneuver and inaccurate actuator-axis knowledge

mechanical prediction could be due to several effects not included. Imprecise knowledge of the fuel location on the spacecraft can introduce large uncertainties in the inertia parameters. Furthermore, as the estimation methods are for a rigid body spacecraft, motion of the fuel mass or any flexible appendages relative to the spacecraft body create a time-varying angular momentum “sink,” whose effects could produce erroneous angular momentum estimates if the motion is of a sufficient magnitude. However, as the mechanical predictions of the MESSENGER spacecraft inertia parameters are still estimates and not necessarily “truth,” the actual error in the estimated states is unknown.

CONCLUSIONS

This paper introduces a substantial modification to existing in-orbit inertia parameter estimation techniques by including the angular momentum of the spacecraft as part of the estimated state. This addition is particularly useful for an on-board recursive implementation of the filter, as it allows for the comparison of a predicted spacecraft angular momentum for a given inertia parameter set to an optimal estimate. As the mechanical alignment of momentum actuators on a spacecraft also contributes to the total system angular momentum, a parameterization of the misalignment error is also included in the estimated state. In addition to an angular momentum-based approach to

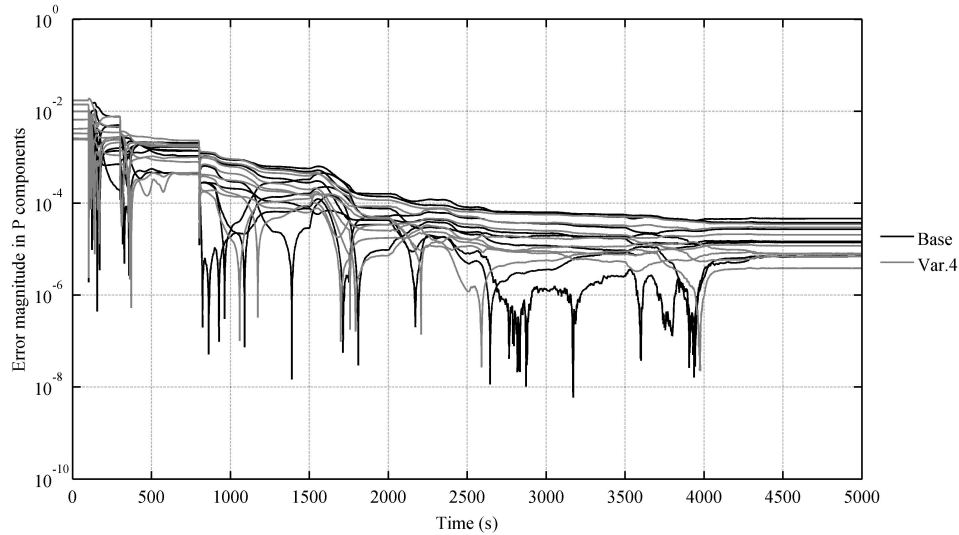


Figure 5. Estimated alignment parameters for simulated maneuver and inaccurate actuator-axis knowledge

inertia parameter estimation, the literature also suggests examining the rotational kinetic energy of the spacecraft as a measurement equation for a filtering scheme. Although using this scalar measurement equation alone does not allow for the inclusion of actuator-alignment parameters as an estimated state, including both kinetic energy and angular momentum measurement equations in the development of the filter makes these parameters observable.

Under simplifying assumptions regarding the torque environment, an estimation scheme based only on an angular momentum measurement equation requires no numerical integration of any of the estimated states, allowing the algorithm to accept infrequent or unevenly-sampled measurements of the spacecraft attitude, angular velocity, and reaction-wheel speeds. Additional artificial process noise affecting the discrete-time dynamics of the angular momentum and inertia parameter states helps compensate for unincorporated, low-magnitude external torques and changes to the physical configuration of the spacecraft. Including kinetic energy as a measurement equation, however, necessitates the numerical integration of the actuator inputs projected onto the spacecraft angular velocity and places more stringent requirements on the sampling frequency of the spacecraft telemetry.

The performance of several parameter estimators including combinations of the angular momentum, kinetic energy, inertia parameter, and alignment parameters states were examined over both a simulated maneuver and using telemetry data during maneuvers of the MESSENGER spacecraft. All filters performed well when the actuator axes were accurately known in the simulated data set, but introduction of actuator alignment error produced significant deviations in the final state estimates of the filters that did not include an actuator-misalignment parameterization as a state. All angular momentum-based filters produced reasonable and consistent estimates of the MESSENGER spacecraft inertia parameters over the four calibration maneuvers examined. The two filters that included actuator-alignment parameters in the estimated state also produced consistent estimates of the actuator axes.

ACKNOWLEDGEMENTS

The work described in this paper was supported by grant 959931 from the Johns Hopkins University Applied Physics Laboratory and contract NAS5-97271 with the National Aeronautics and Space Administration Discovery Program Office.

This material is based on research sponsored by Air Force Research Laboratory under agreement number FA9453-O9-1-0357. The US. Government is authorized to reproduce and distribute reprints for Governmental purposes notwithstanding any copyright notation thereon. The views and conclusions contained herein are those of the authors and should not be interpreted as necessarily representing the official policies or endorsements, either expressed or implied, of Air Force Research Laboratory or the U.S. Government.

NOTATION

a_i	Axis of rotation of the i^{th} reaction wheel in body coordinates $[a_{ix} \ a_{iy} \ a_{iz}]^T$ where T indicates the matrix transpose
\bar{c}	Current best knowledge of arbitrary variable c
f	Discrete-time dynamics function
h	Total angular momentum of a spacecraft in inertial coordinates
H	Discrete-time measurement function
$[I]$	Body-fixed spacecraft inertia matrix
\tilde{I}	Reorganized inertia parameters $[I_{xx} \ I_{yy} \ I_{zz} \ I_{xy} \ I_{xz} \ I_{yz}]^T$ in body coordinates
I_{wi}	Moment of inertia of the i^{th} reaction wheel
$\sum M$	Sum of external torques acting on a rigid body
n	Number of reaction wheels
p_i	two-parameter representation of the alignment error of the i^{th} reaction wheel $[p_{i1} \ p_{i2}]^T$
P	Stacked reaction wheel alignment errors $[p_1^T \ \dots \ p_n^T]^T$
$[{}^a Q^b]$	Direction cosine matrix between coordinate sets a and b . A superscript of N denotes an inertially-fixed coordinate set and k denotes body coordinates at time index k .
T	Rotational kinetic energy of a rigid body
u	Discrete-time dynamics input
v	Discrete-time process noise
w	Discrete-time measurement noise
x,y,z	Spacecraft body axes
x_e	Estimation state
z_e	Discrete-time system measurement. z_h is an angular momentum measurement and z_T is a kinetic energy measurement
$[1_m]$	$m \times m$ identity matrix
Ω	Stacked reaction-wheel speeds $[\Omega_1 \ \dots \ \Omega_n]^T$
ω	Spacecraft body rate expressed in body coordinates
σ	Standard deviation of a random variable

APPENDIX: ACTUATOR-ALIGNMENT ERROR PARAMETERIZATION

The true axis for the i^{th} actuator, a_i , and the best initial estimate of that same axis, \hat{a}_i , are separated by the angle ϕ_i . The corresponding unit-norm axis of rotation, β_i , is by definition perpendicular to both a_i and \hat{a}_i . Representing this rotation as a set of Modified Rodriguez Parameters (MRPs)

allows for the simple description of the actuator-axis alignment error:

$$\rho_i = \beta_i \tan \frac{\phi_i}{4} \quad (16)$$

The rotation matrix corresponding to ρ_i is defined as

$$[Q(\rho_i)] = [1_3] - \frac{4(1 - \rho_i^T \rho_i)}{(1 + \rho_i^T \rho_i)^2} [\rho_i^x] + \frac{8}{(1 + \rho_i^T \rho_i)^2} [\rho_i^x] [\rho_i^x] \quad (17)$$

In general, ρ_i describe a three-parameter representation of the rotation between two sets of coordinates. For the present case of estimating a body-fixed axis, an appropriate choice of these coordinates can further reduce ρ_i to an unambiguous two-parameter set.

Combining the initial estimated actuator axis with two arbitrary, constant, perpendicular directions defines a rotation matrix between actuator and spacecraft body coordinates:

$$[{}^k Q^{gi}] = [\alpha_{1,i} \quad \alpha_{2,i} \quad \hat{a}_i] \quad (18)$$

Because β_i is by definition perpendicular to \hat{a}_i , its representation in the initial “guessed” actuator coordinates consists of only two non-zero parameters:

$$\beta_i = [{}^k Q^{gi}] \begin{bmatrix} b_{1,i} \\ b_{2,i} \\ 0 \end{bmatrix} = [{}^k Q^{gi}] b_i \quad (19)$$

Using b_i instead of β_i to define the MRP set from equation (16) corresponds to defining the actuator-alignment error parameters with respect to the initial guess instead of the spacecraft body coordinates and produces a parameter set with only two non-zero values.

$$\rho_i = \begin{bmatrix} b_{1,i} \\ b_{2,i} \\ 0 \end{bmatrix} \tan \frac{\phi_i}{4} = \begin{bmatrix} p_i \\ 0 \end{bmatrix} \quad (20)$$

The true actuator axis can then be defined in terms of a known $[{}^k Q^{gi}]$ and alignment error parameters p_i with the use of equation (17):

$$a_i = [{}^k Q^{gi}] \left[Q \left(\begin{bmatrix} p_i \\ 0 \end{bmatrix} \right) \right] \begin{bmatrix} 0 \\ 0 \\ 1 \end{bmatrix} \quad (21)$$

Equation (21) can be linearized about a current estimate of the actuator-alignment parameters, \bar{p}_i . Crassidis and Markley provided a compact representation of the linearized effects of variations in a MRP set on a given vector observation.¹⁴ This linearization can be re-interpreted as describing

small variations in the estimated actuator axes:

$$a_i \approx \bar{a}_i + \left[\frac{\partial a_i}{\partial p_i} \right] (p_i - \bar{p}_i) \quad (22)$$

where

$$\bar{a}_i = \begin{bmatrix} k_{Q^{gi}} \end{bmatrix} \begin{bmatrix} Q \left(\begin{bmatrix} \bar{p}_i \\ 0 \end{bmatrix} \right) \end{bmatrix} \begin{bmatrix} 0 \\ 0 \\ 1 \end{bmatrix} \quad (23)$$

$$\left[\frac{\partial a_i}{\partial p_i} \right] = \frac{4}{(1 + \bar{p}_i^T \bar{p}_i)^2} \begin{bmatrix} k_{Q^{gi}} \end{bmatrix} \begin{bmatrix} Q \left(\begin{bmatrix} \bar{p}_i \\ 0 \end{bmatrix} \right) \end{bmatrix} \begin{bmatrix} 0 \\ 0 \\ 1 \end{bmatrix}^x \left((1 - \bar{p}_i^T \bar{p}_i) [1_3] - 2 \begin{bmatrix} \bar{p}_i \\ 0 \end{bmatrix}^x + 2 \begin{bmatrix} \bar{p}_i \bar{p}_i^T \\ 0 \end{bmatrix} \right) \begin{bmatrix} 1 & 0 \\ 0 & 1 \\ 0 & 0 \end{bmatrix} \quad (24)$$

REFERENCES

- [1] E. V. Bergmann, B. K. Walker, and D. R. Levy, "Mass Property Estimation for Control of Asymmetrical Satellites," *Journal of Guidance*, Vol. 10, September-October 1987, pp. 483–491.
- [2] E. Wilson, D. W. Sutter, and R. W. Mah, "Motion-Based Mass- and Thruster-Property Identification for Thruster-Controlled Spacecraft," *Infospace@Aerospace*, No. AIAA-2005-6907, Arlington, VA, AIAA, September 2005.
- [3] J. K. Thienel, R. J. Luquette, and R. M. Sanner, "Estimation of Spacecraft Inertia Parameters," *AIAA Guidance, Navigation, and Control Conference*, No. AIAA-2008-6454, Honolulu, HI, AIAA, August 2008, pp. 1–8.
- [4] A. M. Fosbury and C. K. Nebelecky, "Spacecraft Actuator Alignment Estimation," *AIAA Guidance, Navigation, and Control Conference*, No. AIAA-2009-6316, Chicago, IL, AIAA, August 2009, pp. 1–18.
- [5] S. Tanygin and T. Williams, "Mass Property Estimation using Coasting Maneuvers," *Journal of Guidance, Control, and Dynamics*, Vol. 20, July - August 1997, pp. 625–632.
- [6] M. A. Peck, "Mass-Properties Identification for Spacecraft with Powerful Damping," *Advances in the Astronautical Sciences*, Vol. 103, San Diego, CA, AAS, August 1999, pp. 2005–2024.
- [7] M. A. Peck, "Attitude Determination for Gyrostats in Non-Equilibrium Spins from Infrequent Vector Observations," *AIAA Guidance, Navigation, and Control Conference*, No. AIAA-2000-3946, Denver, CO, AIAA, August 2000, pp. 1–11.
- [8] M. A. Peck, "Attitude Propagation with Intermittent Gyro Measurements and Single-Vector Observations," *AAS/AIAA Astrodynamics Specialist Conference*, No. AIAA-2000-4243, Denver, CO, August 2000, pp. 331–338.
- [9] M. A. Peck, "Estimation of Inertia Parameters for Gyrostats Subject to Gravity-Gradient Torques," *Advances in the Astronautical Sciences*, Vol. 109, San Diego, CA, AAS, August 2001, pp. 113–132.
- [10] A. Y. Lee and J. A. Wertz, "In-Flight Estimation of the Cassini Spacecraft's Inertia Tensor," *Journal of Spacecraft and Rockets*, Vol. 39, January-February 2001, pp. 153–155.
- [11] M. L. Psiaki, "Estimation of a Spacecraft's Attitude Dynamics Parameters by Using Flight Data," *Journal of Guidance, Control, and Dynamics*, Vol. 28, July-August 2005, pp. 594–603.
- [12] Y. Bar-Shalom, X. R. Li, and T. Kirubarajan, *Estimation with Applications to Tracking and Navigation*, p. 481. John Wiley & Sons, 2001.
- [13] M. E. Pittelkau and D. J. O'Shaughnessy, "Gyro Misalignment Decomposition Applied to MESSENGER Calibration," *Advances in the Astronautical Sciences*, Vol. 134, San Diego, CA, AAS, February 2009, pp. 1527–1540.
- [14] J. L. Crassidis and F. L. Markley, "Attitude Estimation Using Modified Rodriguez Parameters," *Proceedings of the Flight Mechanics/Estimation Theory Symposium*, NASA-Goddard Space Flight Center, Greenbelt, MD, May 1996, pp. 71–83.